Improved quantification of Chinese carbon fluxes using CO 2 /CO correlations in Asian outflow

Improved quantification of Chinese carbon fluxes using CO_2/CO correlations in Asian outflow

Parvadha Suntharalingam, Daniel J. Jacob, Paul I. Palmer, Jennifer A. Logan, Robert M. Yantosca, Yaping Xiao, and Mathew J. Evans
Division of Engineering and Applied Sciences, Harvard University, Cambridge, Massachusetts, USA

David G. Streets
Argonne National Laboratory, Argonne, Illinois, USA

Stephanie L. Vay and Glen W. Sachse
NASA Langley Research Center, Virginia, USA

Received 17 November 2003; revised 23 April 2004; accepted 18 May 2004; published 18 September 2004.

[1] We use observed CO_2:CO correlations in Asian outflow from the TRACE-P aircraft campaign (February–April 2001), together with a three-dimensional global chemical transport model (GEOS-CHEM), to constrain specific components of the east Asian CO_2 budget including, in particular, Chinese emissions. The CO_2/CO emission ratio varies with the source of CO_2 (different combustion types versus the terrestrial biosphere) and provides a characteristic signature of source regions and source type. Observed CO_2/CO correlation slopes in east Asian boundary layer outflow display distinct regional signatures ranging from 10–20 mol/mol (outflow from northeast China) to 80 mol/mol (over Japan). Model simulations using best a priori estimates of regional CO_2 and CO sources from *Streets et al.* [2003] (anthropogenic), the CASA model (biospheric), and *Duncan et al.* [2003] (biomass burning) overestimate CO_2 concentrations and CO_2/CO slopes in the boundary layer outflow. Constraints from the CO_2/CO slopes indicate that this must arise from an overestimate of the modeled regional net biospheric CO_2 flux. Our corrected best estimate of the net biospheric source of CO_2 from China for March–April 2001 is 3200 Gg C/d, which represents a 45% reduction of the net flux from the CASA model. Previous analyses of the TRACE-P data had found that anthropogenic Chinese CO emissions must be ~50% higher than in *Streets et al.*'s [2003] inventory. We find that such an adjustment improves the simulation of the CO_2/CO slopes and that it likely represents both an underreporting of sector activity (domestic and industrial combustion) and an underestimate of CO emission factors. Increases in sector activity would imply increases in Chinese anthropogenic CO_2 emissions and would also imply a further reduction of the Chinese biospheric CO_2 source to reconcile simulated and observed CO_2 concentrations. *INDEX TERMS:* 0315 Atmospheric Composition and Structure: Biosphere/atmosphere interactions; 0322 Atmospheric Composition and Structure: Constituent sources and sinks; 0345 Atmospheric Composition and Structure: Pollution—urban and regional (0305); 0365 Atmospheric Composition and Structure: Troposphere—composition and chemistry; *KEYWORDS:* regional carbon fluxes, multiple-species correlations, atmospheric, CO_2 modeling

Citation: Suntharalingam, P., D. J. Jacob, P. I. Palmer, J. A. Logan, R. M. Yantosca, Y. Xiao, M. J. Evans, D. G. Streets, S. L. Vay, and G. W. Sachse (2004), Improved quantification of Chinese carbon fluxes using CO_2/CO correlations in Asian outflow, *J. Geophys. Res.*, *109*, D18S18, doi:10.1029/2003JD004362.

1. Introduction

[2] Inverse model analyses have emerged as an important tool for improving our understanding of the carbon cycle. These analyses have employed atmospheric observations of CO_2 alone [*Bousquet et al.*, 1999; *Fan et al.*, 1998; *Rayner et al.*, 1999], as well as O_2/N_2 ratios [*Keeling et al.*, 1996; *Manning*, 2001; *Bender et al.*, 1996] and $\delta^{13}C$ [*Francey et al.*, 1999] to place constraints on global- and regional-scale carbon exchanges with the atmosphere. They concur on such large-scale features as the existence of significant net terrestrial carbon uptake at northern midlatitudes in the late 1980s and early 1990s [*Bousquet et al.*, 2000, 1999; *Fan et al.*, 1998]. However, they are limited by inadequate observational network coverage [*Gloor et al.*, 2000] and by

0148-0227/04/2003JD004362$09.00

transport model errors [*Gurney et al.*, 2002; *Peylin et al.*, 2002].

[3] Atmospheric CO_2 shares common combustion sources with a number of trace gases, in particular CO. The CO_2/CO emission ratio varies with the efficiency of combustion [e.g., *Andreae and Merlet*, 2001] and thus provides a characteristic signature of source regions and source type. High-resolution measurements of CO_2 and CO are available from a number of aircraft missions but have yet to be exploited for their information on carbon fluxes. In this study we use the distinct and regionally variable CO_2:CO correlations in Asian outflow measured on the TRACE-P aircraft mission [*Jacob et al.*, 2003], together with a global three-dimensional (3-D) model, to explore the regional constraints that they provide on the combustion sources of CO_2 and to separate these contributions from biospheric CO_2 fluxes.

[4] Use of CO to identify combustion and biospheric sources of CO_2 has been demonstrated previously. *Potosnak et al.* [1999], using continuous surface air measurements at Harvard Forest in Massachusetts, employed CO as a predictor of CO_2 emissions from fossil fuel burning in a study of contributions to observed CO_2 variability. A recent analysis by *Langenfelds et al.* [2002] identifies the role of biomass burning in interannual atmospheric CO_2 variations by using flask samples of CO_2, CO, $\delta^{13}C$, and other species from the CSIRO observational network. These studies used isolated surface observations. As we will show here, aircraft observations of CO_2 and CO in continental outflow provide robust information on the diversity of regional signatures.

[5] The TRACE-P campaign, flown from bases in Hong Kong and Yokota (Japan), focused on the quantification of Asian pollution export to the Pacific [*Jacob et al.*, 2003]. Although the aircraft could not fly over land, except for Japan, observations for a range of outflow regions indicated spatially distinct CO_2:CO correlations. The focus of this study is to use these correlations as additional top-down constraints toward obtaining improved estimates of regional CO_2 fluxes. Gridded anthropogenic emission inventories of CO_2 and CO in eastern Asia were generated by *Streets et al.* [2003] to serve as an a priori for the TRACE-P mission. These inventories provide the basis for consistent simulations of combustion in the GEOS-CHEM 3-D chemical transport model (CTM). We analyze these simulations in conjunction with measured concentrations and correlations from the TRACE-P flights to constrain specific components of the east Asian CO_2 budget, including in particular Chinese emissions.

2. TRACE-P Campaign

[6] Measurements in TRACE-P were collected by two research aircraft, a DC-8 and a P-3B, from 24 February to 10 April 2001. Asian outflow to the Pacific in early spring is particularly strong [*Liu et al.*, 2003]. Considerable biomass burning takes place in Southeast Asia during that season and makes a major contribution to the outflow. A detailed overview of mission objectives, flight specifics, and results to date is provided by *Jacob et al.* [2003]. The DC-8 and P-3B had ceilings of 12 and 7 km, respectively. A total of 38 flights were conducted, of which 13 were transit flights from the United States to the western Pacific. We focus here on the western Pacific data (Figure 1) collected from 1 March to 6 April 2001.

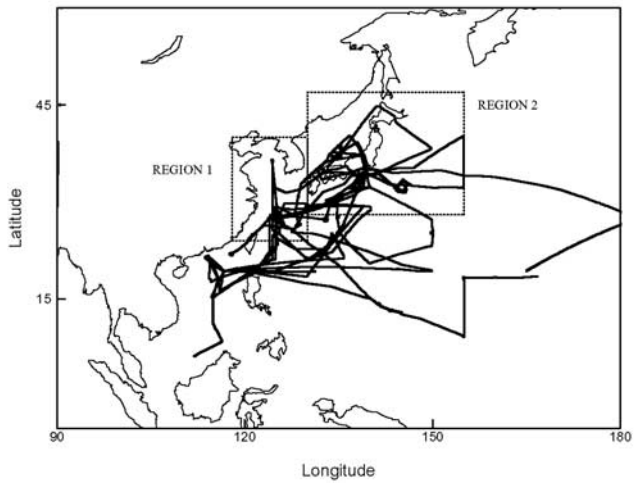

Figure 1. TRACE-P flight tracks off the Asian coast. Also shown are the two regions over which flight data were aggregated for comparisons with model simulations (see section 6.1).

[7] Descriptions of meteorological patterns and outflow pathways during TRACE-P are presented by *Fuelberg et al.* [2003] and *Liu et al.* [2003]. Export of Asian pollution to the Pacific was driven by wave cyclones and the associated cold fronts sweeping across east Asia along a northwest to southeast trajectory. The primary outflow pathways were (1) lifting to the free troposphere in the southwesterly Warm Conveyor Belts (WCBs) ahead of the fronts and (2) post-cold front boundary layer advection [*Cooper et al.*, 2002; *Liu et al.*, 2003]. Lifting of Asian air by the WCBs took place over a wide range of latitudes from 15° to 40°N, resulting in considerable mixing of anthropogenic and biomass burning effluents in the free tropospheric outflow [*Carmichael et al.*, 2003a; *Ma et al.*, 2003; *Miyazaki et al.*, 2003]. In particular, *Hannan et al.* [2003] noted that complex interactions between successive cyclones led to the integration of airstreams ascending from the boundary layer with different histories and pollution signatures. The highest concentrations of CO_2, CO, and other species were sampled in the post-cold front boundary layer outflow off the east coast of China [*Vay et al.*, 2003; *Carmichael et al.*, 2003a; *Bartlett et al.*, 2003; *Simpson et al.*, 2003]. The primary influence here was anthropogenic combustion with less evidence of biomass burning [*Liu et al.*, 2003].

[8] CO_2 measurements were made on both aircraft using nondispersive infrared spectrometers (modified Li-Cor model 6252). Details of measurement procedures are provided in *Anderson et al.* [1996] and the TRACE-P data are presented by *Vay et al.* [2003]. CO was measured using a differential absorption spectroscopic method (DACOM [*Sachse et al.*, 1987]). Analyses of the TRACE-P CO measurements are presented in a number of papers focused on quantifying Asian sources of CO [*Carmichael et al.*, 2003b; *Palmer et al.*, 2003a] or using CO as a tracer of Asian outflow [*Heald et al.*, 2003b; *Russo et al.*, 2003; *Kiley et al.*, 2003; *Palmer et al.*, 2003b]. Our analysis of

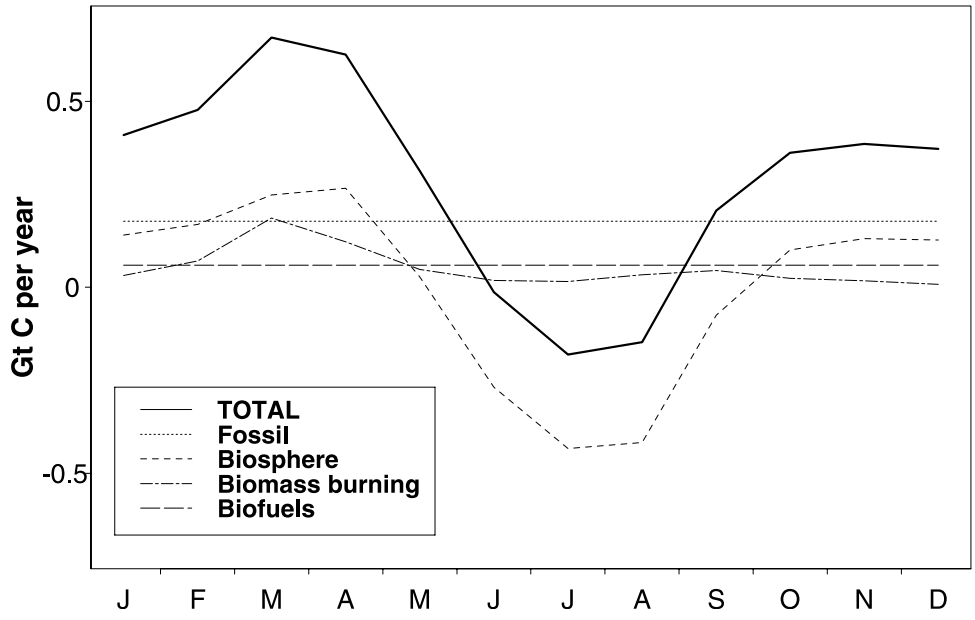

Figure 2. Seasonal variation of east Asian CO_2 surface fluxes derived from the a priori inventories of section 3. East Asia is defined here as the continental domain covered by the regions China, Japan, Korea, India, and Southeast Asia in Figure 3.

CO_2/CO correlations (section 4) uses 1-min averages of the data, and our comparison to CTM simulations in section 6 uses data averaged over the CTM grid and time step resolution ($2^\circ \times 2.5^\circ$ in the horizontal and 48 vertical sigma levels; 15 min).

3. Asian Emission Inventories

[9] The early spring timing of the TRACE-P campaign coincided with the biomass burning season in Southeast Asia [*Duncan et al.*, 2003] and with the seasonal maximum in regional biospheric efflux. In that season, regional CO_2 emission from terrestrial biospheric respiration dominates over photosynthetic uptake. Figure 2 presents the seasonal variation of CO_2 surface fluxes for the east Asian region (aggregated over the ensemble of regions China, Japan, Korea, India, and Southeast Asia in Figure 3) based on a priori inventories presented below. The net source of CO_2 from east Asia is at a maximum in March–April and includes contributions of comparable magnitude from the terrestrial biosphere, fossil fuel combustion, and biomass burning.

[10] The biomass burning contribution is often omitted in long-term analyses of atmospheric CO_2 data. Although it is a large source of CO_2 [*Levine*, 1994], it is largely balanced by vegetation regrowth over the next year [*Houghton and Hackler*, 1999]. Biomass burning does, however, provide an important seasonal source of CO_2 that must be included in analyses of short-term data such as those provided by aircraft campaigns.

[11] *Streets et al.* [2003] developed gridded anthropogenic emission inventories for east Asia, with associated uncertainty estimates, in support of the TRACE-P mission. We rely on this study for the a priori sources of CO_2 and CO from fossil fuel and biofuel. Biomass burning emissions in February–April 2001 were close to the climatological average as indicated by the TOMS Aerosol Index [*Heald et al.*, 2003a]. We use here a global February–April climatology of biomass burning emissions [*Duncan et al.*, 2003], distributed daily on the basis of satellite fire count data for the TRACE-P period [*Heald et al.*, 2003a]. We also account for the small secondary sources of CO from oxidation of anthropogenic and biogenic nonmethane hydrocarbons (NMHCs), which are computed as described by B. N. Duncan et al. (Model study of the variability and trends of carbon monoxide (1988–1997), Model formulation, evaluation and sensitivity, submitted to *Journal of Geophysical Research*, 2003, hereinafter referred to as Duncan et al., submitted manuscript, 2003).

[12] CO_2 exchange with the terrestrial biosphere is based on monthly gridded fields of net primary production (NPP) and heterotrophic respiration provided by the CASA ecosystem model [*Potter et al.*, 1993; *Field et al.*, 1995; *Randerson et al.*, 1997]. The climatological CASA fluxes

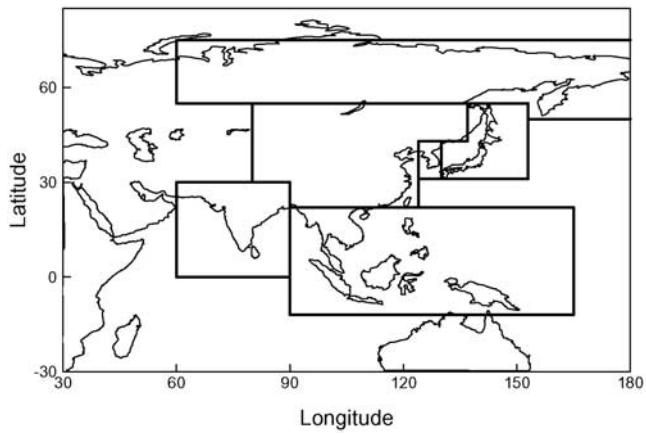

Figure 3. Regions used in the emission inventory analysis: China, Japan, Korea, India, Southeast Asia, and boreal Asia.

Table 1. A Priori East Asian CO_2 and CO Emissions for the TRACE-P Period[a]

	China		Japan		Korea		India		Southeast Asia	
	CO_2	CO	CO_2	CO	CO_2	CO	CO_2	CO	CO_2	CO
Fossil Fuel[b]	1930	75	964	8.2	380	5.8	484	20	686	19
Biofuel[b]	640	53	21	2.3	31	4.7	496	34	314	45
Biomass burning[b]	270	22	11	0.9	4	0.3	552	46	1160	96
Biosphere[c]	5840	4	411	0.5	156	0.1	1080	11	328	31
Totals	8680	154	1410	11.9	571	10.9	2610	111	2490	191

[a]Emissions are in Gg C/d. The a priori estimates of CO_2 and CO fluxes are for the regions of Figure 3. Values are averages for the TRACE-P period (1 March to 6 April 2001).

[b]The combustion sources of CO include a small contribution from oxidation of anthropogenic NMHCs, computed as described by Duncan et al. (submitted manuscript, 2003).

[c]The biospheric flux term for CO_2 represents net emission or the negative of net ecosystem production (NEP), where NEP equals net primary production (NPP) minus emissions from heterotrophic respiration (R_h), as defined by the CASA model [*Randerson et al.*, 1997]. The biospheric source of CO represents production from oxidation of biogenic NMHCs as described by Duncan et al. (submitted manuscript, 2003).

simulate the seasonal cycle of the balanced biosphere (i.e., fluxes at any location integrate to zero over the span of a year). This inventory does not account for CO_2 emissions from biomass burning (which we account for separately as outlined above) or for the subsequent carbon uptake by regrowth. The TRACE-P campaign was conducted before the start of the regional growing season and hence the contribution of this latter component should have little effect on our analysis. We also evaluated a prototype version of the CASA fluxes derived for the year 2001 (J. Randerson and G. van der Werff, personal communication, 2003). Differences between these and the climatological fluxes in the Asian region for the TRACE-P period were small (<2%). We also implemented a version of the CASA fluxes incorporating the diurnal cycle; this is further discussed in section 5. Except for these instances in which specific configurations of the CASA model are evaluated, the biospheric flux inventory in the remainder of this study is that of *Randerson et al.* [1997].

[13] Table 1 presents a breakdown of the a priori CO_2 emissions on a regional and source-specific basis for the TRACE-P measurement period. The regions considered are those of Figure 3. CO_2 emissions from China dominate the east Asian total (55%), and emissions from the biosphere represent 64% of the Chinese total. Biomass burning represents about half of the CO_2 source from Southeast Asia. Fossil fuel combustion is the principal source in Japan and Korea (68% and 66%, respectively). The a priori CO sources are also listed in Table 1. The main regional contributions to atmospheric CO are from Chinese fossil and biofuel combustion and Southeast Asian biomass burning.

[14] Table 2 lists the regional and source-specific CO_2/CO molar emissions ratios derived from these a priori inventories. Regional totals are of most interest as the continental outflow sampled by the aircraft integrates contributions from different processes within a source region. As seen from Table 2, the combustion sources are characterized by a range of ratios that reflect differences in combustion efficiency and in air pollution controls for CO. One can also define a CO_2/CO ratio for the biospheric source on the basis of CO production from short-lived biogenic NMHCs, mainly isoprene. This ratio is generally very high relative to that from combustion (Table 2). Southeast Asia is an exception with a low value of 11. In this tropical region, the opposing NPP and respiration fluxes of CO_2 are large and almost equal, yielding an NEP flux close to zero. The combination of low NEP CO_2 emissions and high production of CO from local biogenic NMHC emissions results in the low biospheric CO_2/CO ratio.

[15] The overall CO_2/CO source signature of a region is then determined by the relative proportions of the different sources. In China, the low-efficiency biomass combustion sources display low CO_2/CO emission ratios of ~12 (mol/mol), whereas fossil fuel combustion has an emission ratio of 26. The overall ratio for China is 56, reflecting a major contribution from the terrestrial biosphere. In Japan, air pollution controls for CO result in a high fossil fuel ratio of 117. Contributions from biomass burning and biofuel use are relatively small there, as is the biospheric flux. This results in an overall Japanese CO_2/CO ratio of 122, a factor of 2 higher than for China. The lowest CO_2/CO emission ratios are for India and Southeast Asia, reflecting the major influences of biomass burning and biofuel combustion in these regions.

4. Observed CO_2/CO Correlations and Relationships to Sources

[16] We illustrate some of the distinct regional signatures seen in the TRACE-P CO_2/CO correlations by using data from two flights in conjunction with back trajectory calculations from *Fuelberg et al.* [2003]. The CO_2/CO slopes in this analysis and in the remainder of the study are obtained using the reduced major axis method [*Hirsch and Gilroy*, 1984]. This method estimates the linear relationship between two variables by minimizing the residual variance in x and y directions (rather than just the y dimension as in standard linear regression); hence it is preferable for determining the CO_2:CO correlations in our analysis.

4.1. DC-8 Flight 16 (29 March 2001)

[17] Figure 4 shows the CO_2/CO relationships observed on DC-8 flight 16. This was a sunrise flight that ascended out of Yokota Air Force Base, Tokyo, and made repeated measurements of the same vertical profile over the East China Sea (124°–125°E, 28.5°N) before returning to Japan.

Table 2. A Priori East Asian CO_2/CO Molar Emission Ratios[a]

	China	Japan	Korea	India	Southeast Asia
Fossil fuel	26	117	65	24	36
Biofuel	12	9.1	6.6	15	7.0
Biomass burning	12	12	12	12	12
Biosphere[b]	1460	822	1560	98	10.6
Regional average	56	119	52	24	13

[a]Ratios are derived from the a priori inventories of Table 1 for the period March to 6 April 2001.

[b]A combination of high biogenic NMHC emissions and small NEP CO_2 fluxes explains the low biospheric CO_2/CO emissions ratio for Southeast Asia.

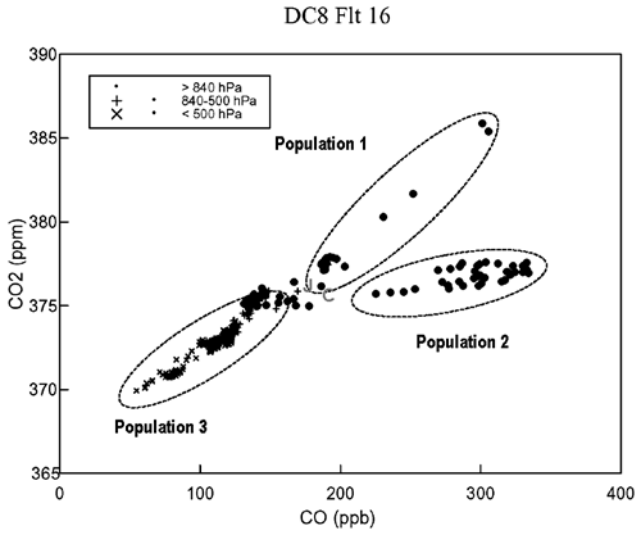

Figure 4. CO_2/CO correlations measured on DC8 flight 16 out of Yokota Air Force Base, Japan (29 March 2001). Mean slopes for the different populations are 65 for population 1 (boundary layer ascent out of Japan), 12 for population 2 (boundary layer outflow from China), and 60 for population 3 (midtropospheric background). Also included on plot are the local background concentrations in the boundary layer of region 1 (C) and region 2 (J).

The aircraft sampled a heavy Chinese pollution plume in the boundary layer, capped by clean subsiding air in the free troposphere above 2 km. The CO_2/CO slopes in Figure 4 show three distinct populations which we discuss in turn:

[18] Population 1 is the ascent out of Tokyo (surface to 3 km). The CO_2/CO slope of 65 mol/mol is at the high end of the range observed in the boundary layer during TRACE-P. Emission inventories indicate a Japanese CO_2/CO source signature of 122 (Table 2). The CO_2/CO slope measured here is ~40% lower. Other analyses of TRACE-P boundary layer measurements over Japan point to the influence of transport from Korean and Chinese sources upwind [*Palmer et al.*, 2003b; *Blake et al.*, 2003], and this could explain the discrepancy. We will return to this point later.

[19] Population 2 is the Chinese boundary layer outflow. The CO_2/CO slope is only 12 mol/mol. Back trajectories indicate a dominant influence from the Shanghai region. The CO_2/CO slope is typical of biofuel or biomass burning and much lower than would be expected regionally for China (Table 2). On the basis of their analysis of TRACE-P flights over the East China and Yellow Seas, *Carmichael et al.* [2003a] concluded that Chinese domestic fuel emissions for CO in *Streets et al.*'s [2003] inventory are greatly underestimated. Such a source would be expected to have a low CO_2/CO emission ratio. Again, we will return to this point later.

[20] Population 3 is the background free tropospheric air. Concentrations are low and the CO_2/CO slope is 60 mol/mol. Correlation between CO_2 and CO would be expected to reflect the common large-scale latitudinal gradients of the two gases during that season. This is consistent with our global CTM simulation for the TRACE-P period (section 5), which indicates a mean CO_2/CO correlation slope of 72 in free tropospheric background air upstream of east Asia.

4.2. P-3B Flight 14 (18 March 2001)

[21] This flight sampled boundary layer outflow south of Japan and over the Yellow Sea, downwind of northern China and Korea. The outflow was capped by a strong subsidence inversion at 2 km altitude. As seen in Figure 5, the CO_2/CO correlations measured on this flight fall into distinct populations.

[22] Population 1 is the boundary layer outflow sampled south of Japan. This population is characterized by a high CO_2/CO slope of 75. Back trajectories indicate boundary layer influences from the Chinese coastal region between Shanghai and Qingdao, as well from South Korea and the southern tip of Japan. *Blake et al.* [2003] find a strong Korean and Japanese influence on these flight legs as indicated by high levels of methyl bromide. This could explain the high CO_2/CO slope.

[23] Population 2 is the Chinese boundary layer outflow over the Yellow Sea. The CO_2/CO slope is 22. The CO measurements are some of the highest in the campaign. Back trajectories indicate surface influence from the Beijing/Tianjin region as well as further south toward Qingdao. Characteristics of these plumes are discussed by *Weber et al.* [2003] and *Carmichael et al.* [2003a]. As with population 2 from DC-8 flight 16, the low CO_2/CO slope could result from domestic combustion sources.

[24] Population 3 is the subsiding air at 2–3 km altitude. This population displays a high CO_2/CO slope (80) typical of the free tropospheric background discussed previously.

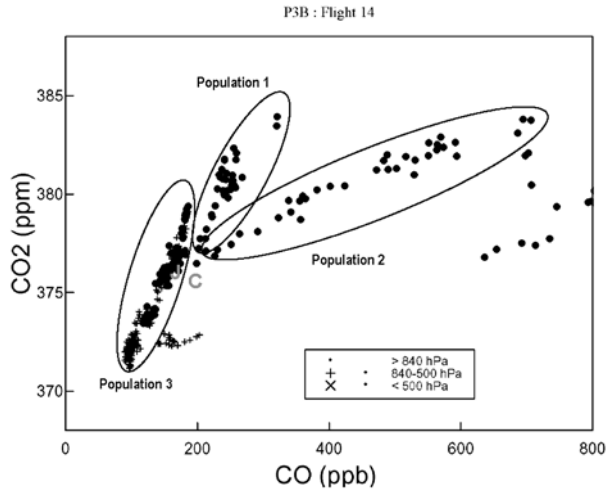

Figure 5. CO_2/CO correlations measured on P3B flight 14 over the Yellow Sea (18 March 2001). Mean slopes for the different populations are 75 for population 1 (mixed boundary layer outflow from China, Korea and Japan), 22 for population 2 (boundary layer outflow from northeast China), and 80 for population 3 (midtropospheric background air). The measurements characterized by high CO (>600 ppbv) that are not included in population 2 are from the Beijing urban plume. Also included on plot are the local background concentrations in the boundary layer of region 1 (C) and region 2 (J).

[25] In subsequent analysis we focus on the well-defined boundary layer CO_2/CO slopes apparent in these and other TRACE-P flights (e.g., Figures 4 and 5). These measurements predominantly sampled the post-cold front airstream in the boundary layer associated with the passage of cyclones across the east Asian continent [*Cooper et al.*, 2002; *Liu et al.*, 2003; *Fuelberg et al.*, 2003]. For species such as CO_2 and CO, for which the background mixing ratio varies regionally, the correlation slopes reflect dilution with the local background (lower left of slope) as well the emissions ratio signature of surface fluxes (upper right of slope) [*McKeen and Liu*, 1993; *Mauzerall et al.*, 1998]. Differences between observed correlation slope and surface emission ratio depend on the discrepancy between the local background concentration and that at the emissions location [e.g., see *Mauzerall et al.*, 1998, Figure 4b]. Back trajectory analysis of the measurements defining the boundary layer slopes in Figures 4 and 5 indicates that these air masses traversed the polluted boundary over northeast China, Japan, and Korea, and were sampled less than 1 day's travel time from surface emissions influence [*Fuelberg et al.*, 2003]. The local background at these measurement locations will, therefore, not differ significantly from that at the emissions location, and the observed slopes predominantly reflect the influence of surface emissions. The TRACE-P campaign did not include flights over the east Asian mainland making identification of local background concentrations at the emissions source and in upstream regions difficult. In Figures 4 and 5 we include the local background concentrations in the boundary layer of regions 1 and 2. The local background is derived as a low percentile of boundary layer measurements, over all the TRACE-P flights in the region, using the methodology of *Mauzerall et al.* [1998]. The 10th percentile values are 375.3 ppm for CO_2 and 203.4 ppb for CO for the region 1 boundary layer (symbol C), and 375.6 ppm (CO_2) and 167.3 ppb (CO) for region 2 (symbol J). The differences in local background are not large across these regional scales, suggesting that the primary influence on the observed boundary layer slopes are the local emissions and not variations in background conditions.

5. Global Model Simulation of CO_2 and CO for the TRACE-P Period

[26] Quantitative interpretation of the observed CO_2/CO slopes in terms of their constraints on sources requires a 3-D model to resolve the effects of transport and associated mixing of different source types and source regions. We simulate CO_2 and CO with the GEOS-CHEM CTM (version 4.33) driven by assimilated meteorological observations from the Goddard Earth Observation System (GEOS) of the NASA Global Modeling and Assimilation Office (GMAO). The horizontal resolution is $2^\circ \times 2.5^\circ$ with 48 vertical sigma levels and a dynamic time step of 15 min. The original description of the GEOS-CHEM CTM is given by *Bey et al.* [2001]. Applications of the CO simulation for the TRACE-P period to constrain east Asian fossil fuel and biomass burning emissions are presented by *Palmer et al.* [2003a] and *Heald et al.* [2003b]. Further applications of GEOS-CHEM to the interpretation of CO data from TRACE-P are presented by *Li et al.* [2003], *Liu et al.* [2003], and *Jaeglé et al.* [2003]. *Kiley et al.* [2003] have evaluated the GEOS-CHEM CO simulation against the TRACE-P observations and find no overall bias in model simulated transport. For their inverse analysis of TRACE-P CO observations, *Palmer et al.* [2003a] estimated a distribution of transport error for the GEOS-CHEM CO simulation. Their methodology was based on statistics of the differences between aircraft measurements and model simulations, and it accounted for model bias in simulated concentrations due to emissions error. They estimated relative errors due to transport of 20–30% in the TRACE-P domain. We further discuss the role of transport error and implications for our analysis in section 6.

[27] Simulation of CO_2 is a new GEOS-CHEM capability that draws on our previous CO_2 simulation with the GISS II' CTM [*Suntharalingam et al.*, 2003]. We have evaluated the global characteristics of the GEOS-CHEM CO_2 simulation (surface distributions and detrended seasonal cycles) using data from GLOBALVIEW-CO_2 [*Climate Monitoring and Diagnostics Laboratory* (*CMDL*), 2003]. The modeled distribution reproduces the observed large-scale spatial gradients, as well as the amplitude and phasing of the seasonal cycle at most of the observation sites. For the TRACE-P simulations, we combine the regional Asian emission inventories of CO_2, discussed in section 3, with standard global inventories for the rest of the world in 2001. These include CO_2 fluxes from fossil fuel combustion (G. Marland et al., Global, regional, and national CO_2 emissions, in Trends: A Compendium of Data on Global Change, 2001, available at http://cdiac.esd.ornl.gov/trends/emis/meth_reg.htm), biofuel combustion [*Yevich and Logan*, 2003], biomass burning [*Duncan et al.*, 2003], seasonal exchange with the terrestrial biosphere (CASA model [*Potter et al.*, 1993; *Field et al.*, 1995; *Randerson et al.*, 1997]), and air-sea fluxes (gridded database of *Takahashi et al.* [1999]). The variability of CO_2 concentrations in the TRACE-P flight region is determined by combustion sources and the terrestrial biosphere, with negligible contribution from the ocean. We do not discuss further the role of ocean exchange in this study.

[28] The CASA fluxes employed here are driven by climatological Normalized Difference Vegetation Index (NDVI) products and mean temperature and precipitation distributions [*Randerson et al.*, 1997; *Potter et al.*, 1993]. Fluxes derived for the year 2001 (J. Randerson and G. van der Werff, personal communication, 2003), yield similar values for the China region (5920 Gg C/d) as the climatology (5840 Gg C/d). These CASA fluxes do not resolve the diurnal variation of terrestrial biospheric CO_2 emissions. We evaluated the resulting error in our analysis of TRACE-P aircraft data by testing a prototype version of the CASA fluxes that accounts for diurnal variation [*Olsen and Randerson*, 2004]. The resulting effects were not significant, which can be explained by the small amplitude of the diurnal cycle in the CASA fluxes for temperate Asia in February–April, and by the 1–2 day oceanic fetch of the continental outflow sampled in TRACE-P [*Fuelberg et al.*, 2003].

[29] The CO_2 simulation was spun up from 1 January 2000 and run for 16 months to the end of April 2001. Because of the omission of net uptake by the land biosphere during the period of spin-up, modeled CO_2 concentrations display a small positive bias, relative to observations, at the

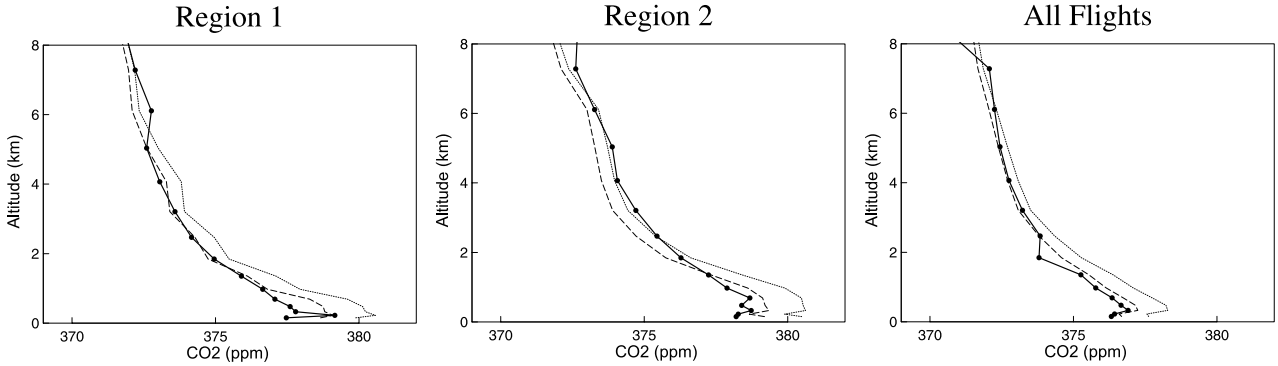

Figure 6. Mean variation of CO_2 concentrations with altitude along the TRACE-P flight tracks, for regions 1 and 2 and for the ensemble of flights west of 150°E. The aircraft observations (bold line) are compared to GEOS-CHEM model results using the a priori scenario emissions inventories (dotted line) and the optimized decreased biosphere emission scenario of section 6.2 (dashed line).

beginning of the TRACE-P simulation (1 March 2001). The modeled distribution is therefore adjusted downward, with a single global subtraction, to eliminate this bias and to match observations from the GLOBALVIEW-CO_2 [*CMDL*, 2003] database at the start of the TRACE-P period. We employ this bias elimination to ensure that omissions and errors in the emissions inventories during the model spin-up prior to the start of the TRACE-P do not have an impact on the analysis for the March–April 2001 period. Our a priori CO simulation is that reported by *Palmer et al.* [2003a]. It includes the a priori Asian CO emission inventories for fuel combustion and biomass burning from *Streets et al.* [2003] and *Heald et al.* [2003a], respectively. Chemical sources of CO include oxidation of methane and NMHCS as described by Duncan et al. (submitted manuscript, 2003). Loss of CO by oxidation is computed using archived 3-D OH concentration fields from a GEOS-CHEM tropospheric chemistry simulation [*Martin et al.*, 2003]. We also consider, in section 6.3, the a posteriori CO simulation of *Palmer et al.* [2003a], where the source estimates have been adjusted using an inverse analysis of the TRACE-P CO measurements. The main changes relative to the a priori simulation are a 54% increase in anthropogenic Chinese emissions and a 74% decrease in biomass burning in Southeast Asia. These findings on fossil emissions are consistent with earlier studies reporting an underestimate of Asian CO sources based on inverse analyses of CO measurements from the NOAA CMDL flask network [*Kasibhatla et al.*, 2002; *Pétron et al.*, 2002].

6. Interpretation of CO_2/CO Correlations in TRACE-P

6.1. Simulations Based on a Priori Inventories

[30] Our analysis of CO_2-CO relationships in Asian outflow during TRACE-P focuses on boundary layer observations (>840 hPa) in two regions: off-shore China (region 1) and over Japan (region 2) (Figure 1). We chose to focus on these regions as they were determined to be the most strongly influenced by Asian CO_2 and CO outflow [*Vay et al.*, 2003; *Carmichael et al.*, 2003a]. To compare model and observations, we averaged the 1-min merged data for TRACE-P CO_2 and CO measurements over the model grid resolution (2° × 2.5°and 48 vertical levels) and time step. The model simulations were sampled along the flight tracks. Figures 6 and 7present the mean vertical profiles of observed and simulated concentrations of CO_2 and CO. The CO_2 simulation is too high in the boundary layer by 1.9 ppmv for the outflow regions 1 and 2 (China and Japan). The model CO is too low, by 23 ppbv for the ensemble of data

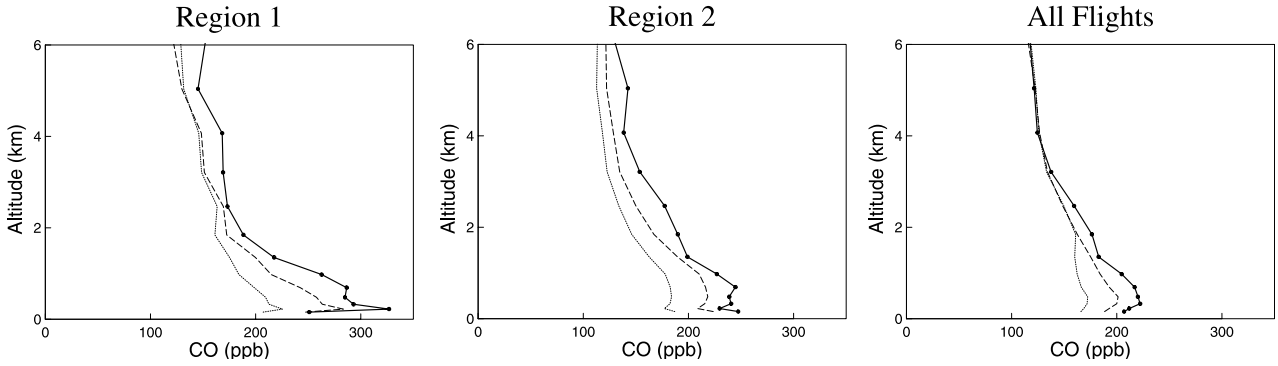

Figure 7. Mean variation of CO concentrations with altitude along the TRACE-P flight tracks, for regions 1 and 2 and for the ensemble of flights west of 150°E. The aircraft observations (bold line) are compared to GEOS-CHEM model results using the a priori emissions inventories (dotted line) and the optimized a posteriori estimates of *Palmer et al.* [2003a] (dashed line).

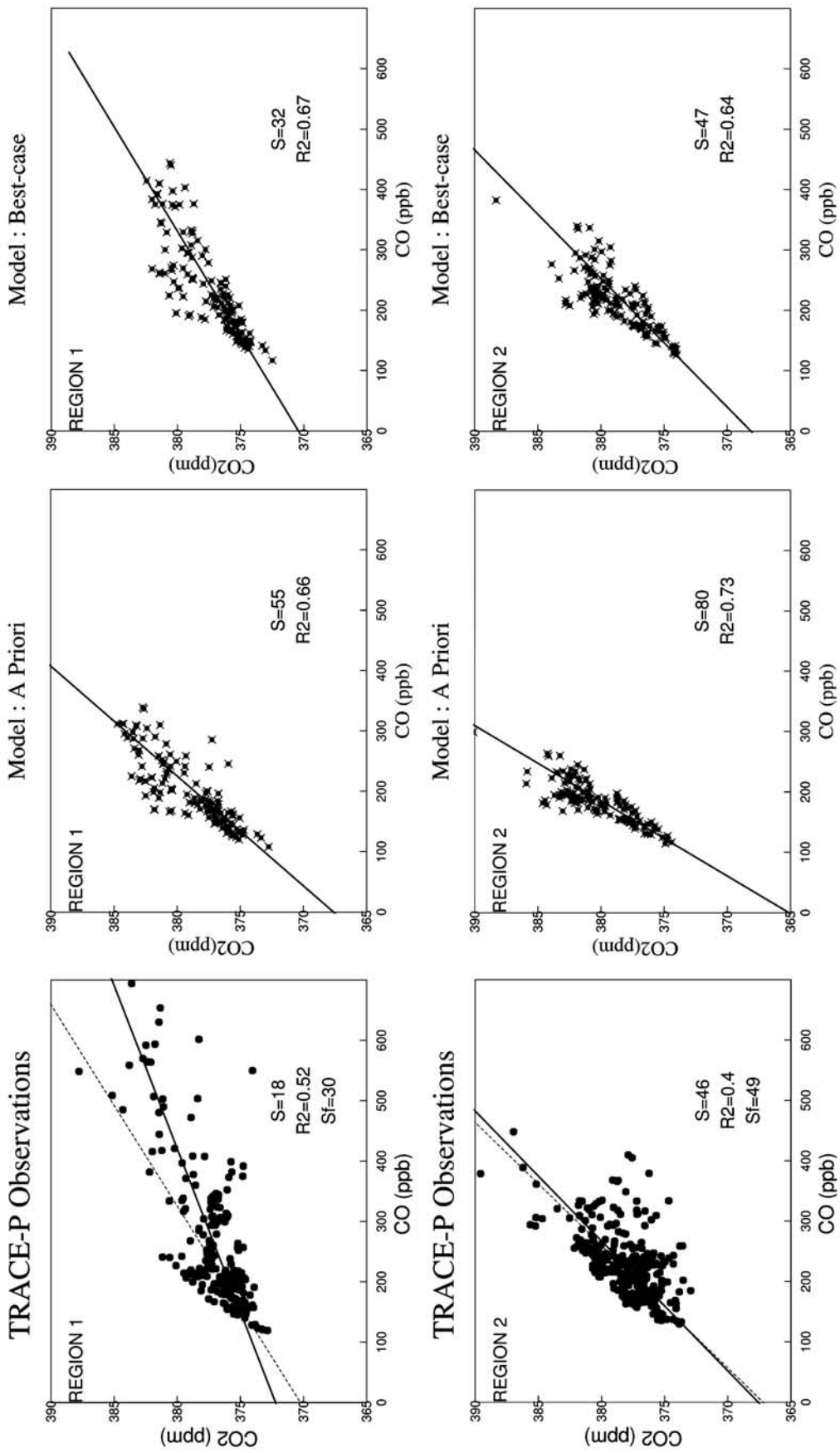

Figure 8. Comparison of boundary layer (>840 hPa) CO_2:CO correlations in regions 1 and 2 from (left) TRACE-P observations and (middle) GEOS-CHEM simulations for a priori inventories, and (right) our best-case scenario decreased biosphere/a posteriori CO. The model is sampled along the aircraft flight tracks. The RMA linear regression with slope S is plotted (solid line). Also shown is the RMA regression slope, S_f (dotted line), when the TRACE-P CO observations are filtered to remove outliers, as in the analysis of *Palmer et al.* [2003a].

and by more in the boundary layer, due to an underestimate of anthropogenic sources in China [*Palmer et al.*, 2003a].

[31] In deriving a diagnostic to evaluate regionally aggregated CO_2/CO correlations we also considered such options as (1) CO_2 and CO enhancements above background levels (ΔCO_2, ΔCO) and (2) correlation "envelopes" to account for the range of correlation slopes within a region. We finally settled on the method of linear regression slopes as the most robust method for implementing a comparison between model and observations; the method of CO_2 and CO enhancements, for example, can be sensitive to the definition of the local background value.

[32] Boundary layer linear regression slopes from model and observations are shown in Figure 8. Mean CO_2/CO slopes were derived using the reduced major axis method [*Hirsch and Gilroy*, 1984] and are presented in Table 3 (as the "a priori" scenario). The mean observed values differ by more than a factor of 2 between region 1 (18) and region 2 (46). This is consistent with greater Japanese influence in region 2. The model slopes generated from a priori source inventories are too high, by almost a factor of 3 for region 1 and a factor of 2 for region 2, which reflects the model overestimate of CO_2 concentrations and the model underestimate of CO (Figures 6 and 7). We find that within the model world, the boundary layer CO_2/CO slopes are consistent with regional source ratios (e.g., in region 1, the model slope of 55 (Table 3) matches the a priori Chinese source ratio of 56 (Table 2)).

[33] Discrepancies between modeled and observed concentrations and CO_2/CO slopes could arise from errors in a priori inventories or in model transport. We first consider the accuracy of modeled transport. *Kiley et al.* [2003] have evaluated the GEOS-CHEM CO simulation in a transport model intercomparison study of the TRACE-P campaign. The most significant GEOS-CHEM transport errors were found to be excessive model convection over regions of Southeast Asia and eastern India. *Kiley et al.* [2003] also evaluated the modeled simulation of planetary boundary layer (PBL) depth in the high anthropogenic emissions region of northeast China. The PBL depth here is an important determinant of the accuracy of modeled concentrations in boundary layer outflow in regions 1 and 2. They concluded that the GEOS-CHEM model accurately simulated characteristics of the shallow PBL in this region. We therefore ascribe the discrepancies between modeled and observed concentrations in the offshore Asian boundary layer primarily to errors in a priori inventories.

Table 3. CO_2:CO Correlation Slopes (mol/mol) and R^2 Along the TRACE-P Flight Tracks[a]

		Model		
Region	Observations[b]	A Priori	Decreased Biosphere	Decreased Biosphere/ A Posteriori CO
Region 1: China outflow (>840 hPa)				
Slope	18 (30)	55	46	32
R^2	0.52	0.66	0.65	0.67
Region 2: Japan outflow (>840 hPa)				
Slope	46 (49)	80	69	47
R^2	0.4	0.73	0.72	0.64

[a]The comparisons are for the regions of Figure 1. The mean CO_2/CO slopes are derived by linear regression using the reduced major axis method on each set of regional data. The a priori model simulation uses the CO_2 and CO inventories of Table 1. The decreased biosphere simulation imposes a reduction of net biospheric CO_2 emissions (45% in China and 10% in boreal Asia). The decreased biosphere/a posteriori CO simulation includes, in addition, the a posteriori CO emissions estimates of *Palmer et al.* [2003a] and achieves the closest agreement to the observed CO_2/CO slopes.

[b]Values in parentheses represent the mean CO_2/CO slopes obtained when CO observations are filtered to remove outliers as was done in *Palmer et al.*'s [2003a] analysis.

6.2. Constraints on CO_2 Emissions Using CO_2/CO Slopes

[34] In this section we combine the simulations of CO_2, CO, and CO_2/CO slopes to obtain top-down constraints on Asian CO_2 emissions. We previously showed that the model with a priori source estimates overestimates CO_2 concentrations in the boundary layer with the largest discrepancy apparent in Chinese outflow. Reconciliation of modeled CO_2/CO slopes and mean CO_2 concentrations with the observations specifically requires a reduction in a regional CO_2 source with a CO_2/CO source ratio higher than the regional model mean value of 55. Among the Chinese CO_2 sources of Table 1, the only one that meets this criterion is the terrestrial biospheric flux. Decreases in net biospheric emissions of 45% for China (from 5840 to 3210 Gg C/d) and 10% for boreal Asia (defined as the Asian landmass east of 60°E and north of 55°N) give a better match between modeled and observed CO_2 in regions 1 and 2 and represent the "decreased biosphere" scenario in Figure 6. These CO_2 emission changes eliminate the boundary layer overestimate of the CO_2 observations in all regions (Figure 6). They also decrease the modeled CO_2/CO slopes (Table 3) but not sufficiently to match the observed slopes. An increase in CO emissions is further required and will be discussed later.

[35] We focus primarily on Chinese emissions in this analysis. As noted previously, a number of TRACE-P studies attribute the elevated concentrations of CO_2 and CO observed in this boundary layer region to outflow from the Chinese mainland. We further found, using regionally "tagged" GEOS-CHEM simulations (based on the regions of Figure 2), that emissions from the Chinese region provided the dominant influence in the region 1 boundary layer. Emissions from the other upstream regions exerted little influence on modeled CO_2 concentrations here, and emissions adjustments in these regions to match observed boundary layer concentrations in region 1 resulted in a degradation of the modeled CO_2 simulation in other parts of the TRACE-P domain. An optimal set of regional emissions adjustments requires a formal inversion which will be carried out as the next step of this analysis.

[36] The net biospheric flux in the model represents the balance between two large modeled fluxes defined by the CASA model (CO_2 uptake from NPP and emission from heterotrophic respiration) and is subject to some uncertainty. For the seasonal TRANSCOM inversions, *Gurney et al.* [2004] employ prior uncertainties on the CASA net biospheric fluxes in temperate Asia of 2.0, 2.2, and 2.5 Gt C/yr for February, March, and April, respectively (equivalent to 73%, 80%, and 92% of the net biospheric flux). Our 45% adjustment of the net biospheric source from China is within

this range of uncertainty. However, matching the observed CO_2/CO slope of 18 in China outflow (region 1, boundary layer), would require a decrease in Chinese biospheric emissions of almost 200% (i.e., China would have a net biospheric uptake of 5800 Gg C/d for the TRACE-P period). Such a change would be outside the estimated range of uncertainty on the a priori, and it would reduce the mean modeled CO_2 in the region 1 boundary layer to 374.8 ppmv, a value much lower than observed (377.1 ppmv).

[37] Since consistency between observed and modeled CO_2/CO slopes is not achievable through further reduction of CO_2 emissions, error in a priori emission estimates for CO, as previously identified by *Carmichael et al.* [2003b] and *Palmer et al.* [2003a], is a likely explanation. *Streets et al.* [2003] note a possible underestimate of biofuel or domestic coal emissions in their CO inventory due to underreporting of domestic coal use in rural central China. Their stated uncertainty (95% confidence level) for Chinese fuel CO emissions (156%) is significantly larger than the corresponding uncertainty on Chinese fuel CO_2 emissions (16%).

[38] Inverse modeling of the TRACE-P CO observations, using GEOS-CHEM as the forward model, calls for a 54% increase in Chinese fuel CO emissions relative to the *Streets et al.* [2003] a priori and a 74% decrease in Southeast Asian emissions relative to the *Duncan et al.* [2003] a priori, with smaller changes for the other CO sources [*Palmer et al.*, 2003a]. Figure 7 shows the resulting vertical profiles. There is still a low bias in the CO simulation, in part because large transport errors were assigned to the simulation of urban plumes observed in the boundary layer outflow. Including the a posteriori CO emission estimates of *Palmer et al.* [2003a] in our analysis (new model scenario ''decreased biosphere/a posteriori CO'') further decreases modeled CO_2/CO slopes in the boundary layer to 32 in region 1 and 47 in region 2 (Table 3). While the modeled slope in region 2 (47) is now close to the observed boundary layer value of 46, the slope in region 1 (32) is still higher than the observed value of 18; this difference may result from the inability of the model to simulate observed urban plumes with high CO. We note that filtering the CO measurements to remove the influence of outliers as was done in the *Palmer et al.* [2003a] analysis, results in an observed boundary layer slope in region 1 of 30 mol/mol (Figure 8), yielding a better match between observations and the decreased biosphere/a posteriori CO scenario.

6.3. Implications of the a Posteriori CO Simulation for Asian CO_2 Emissions

[39] The large adjustments to the Chinese and biomass burning CO sources in the TRACE-P inverse model analysis of *Palmer et al.* [2003b] raise the question as to the implications for CO_2. *Streets et al.* [2003] construct bottom-up combustion inventories for CO and CO_2 by applying species-specific emission factors to common databases of activity rates (and abatement technologies when relevant). The activity rates represent rates of fuel consumption, and emission factors are defined as mass of the trace gas (grams) per kilogram of fuel combusted [*Streets et al.*, 2003, Table 4]. The errors in the a priori inventories for CO could be due to errors in activity rates, which would have associated implications for CO_2 emissions, or in CO emission factors, which would not.

Table 4. Chinese Fuel CO_2 and CO Emissions by Sector in *Streets et al.*'s [2003] Inventory[a]

	Domestic					
	Biofuel	Coal	Industry	Transport	Power[b]	Cement
CO_2, Gg C/d	556	181	809	228	710	156
CO, Gg C/d	42	9.6	21	45	-	-
CO_2/CO, mol/mol	13	19	38	5.1		

[a]Small differences between these totals and those of Table 1 are due to different regional definitions for China. The numbers here are computed for the Chinese region defined by *Streets et al.* [2003]. The fluxes of Table 1 are computed for the regions of Figure 3.

[b]*Streets et al.* [2003] assumed western emissions controls standards for the power plants included in their analysis and hence estimate negligible CO emissions from this sector.

[40] We first examine the Chinese anthropogenic sector, for which *Palmer et al.* [2003b] adjusted CO emission upward by 54% relative to the a priori of *Streets et al.* [2003]. Uncertainties given by *Streets et al.* [2003] on their Chinese fuel inventories are 156% for CO and 16% for CO_2, and Table 4 presents their partitioning of Chinese fuel emissions among the main sectors. The CO_2/CO emissions ratios, aggregated for each sector, vary from 5 mol/mol (transport) to 38 mol/mol (industry). *Streets et al.* [2003] assumed western emissions controls standards for the power plants included in their analysis and hence estimate negligible CO emissions from this sector.

[41] Likely candidates for the underestimate in CO emissions are the domestic coal and biofuel sectors [*Carmichael et al.*, 2003b] and small heavily polluting power plants unaccounted for in official industry statistics [*Bradsher*, 2003]. We consider first the possibility of an underestimate in the domestic fuel sector activity with two extreme scenarios, ''increased domestic coal'' and ''increased biofuel'', for which the CO underestimate derives entirely from these subsectors. Our analysis approach here is to estimate the changes in sector activity based on the projected increase in CO emissions from *Palmer et al.* [2003a], and then derive consistent CO_2 emissions changes. The implied increases in activity rates are a factor of 7.5 for the domestic coal sector (equivalent to CO_2 emissions increasing from 181 to 1370 Gg C/d), or 2.5 for the biofuels sector (equivalent to CO_2 emissions increasing from 556 to 1396 Gg C/d). These changes in CO_2 (32% to 45% of Chinese anthropogenic emissions) fall outside the 16% uncertainty estimated by *Streets et al.* [2003].

[42] Implementation of these CO_2 emissions in the GEOS-CHEM model leads to a mean overestimate of CO_2 concentration in the boundary layer of region 1 by 1.2 ppm (increased biofuel) and 1.3 ppm (increased domestic coal). The corresponding mean CO_2/CO slopes are 35 and 37 mol/mol which degrade the simulation of observations relative to the decreased biosphere/a posteriori CO scenario of section 6.2. Reconciliation of simulated boundary layer CO_2 with the observations, for the increased biofuel scenario, for example, would require further decreases in the Chinese biospheric flux (of 1200 Gg C/d). The overall required decrease in the Chinese biospheric flux would thus be 3800 Gg C/d (also accounting for the contribution from the decreased bio-

sphere scenario) and equivalent to 65% of net Chinese biospheric emissions. We note, however, that such an adjustment would still be within the uncertainty bounds on the springtime CASA fluxes from *Gurney et al.* [2004].

[43] We next consider the possibility of errors in CO emission factors, rather than sector activity rates, as being responsible for the underestimate of Chinese CO fuel emissions. Under this assumption, attribution of the CO emissions adjustment implied by *Palmer et al.* [2003b] to the domestic fuel subsectors would result in unrealistically high CO emission factors, 15% CO for biofuels, or 29% for domestic coal.

[44] Unaccounted CO emissions from older heavily polluting power plants, designated for closure but apparently still active [*Bradsher*, 2003], is another possibility. While modern power plants are equipped with emissions controls designed to minimize CO emissions, older plants lacking this technology, may provide a significant source of CO. *Streets et al.* [2003] do not account for such plants in their analysis. If the underestimate of Chinese anthropogenic CO emissions were due solely to this source then the overall CO emission factor for the power plant sector (assuming no increase in CO_2 emission) would be 8%, which again seems unrealistically high.

[45] It appears therefore that no single factor can easily explain the underestimate of anthropogenic Chinese CO emissions in *Streets et al.*'s [2003] inventory. A multiple explanation, involving a combination of underreporting of sector activity together with low bias in CO emission factors, seems most likely. The former would imply a reduction in the biospheric source of CO_2 beyond that used in our decreased biosphere/a posteriori CO scenario but still within the uncertainty range estimate of *Gurney et al.* [2002] for the springtime CASA fluxes.

[46] We now examine the consequences of the large decrease in biomass burning CO emissions (−74% relative to the a priori in Southeast Asia) estimated by *Palmer et al.* [2003a]. If this were due to an overestimate of biomass burning activity (as opposed to an overestimate in emission factor) then CO_2 emissions should correspondingly decrease. We focus on the free troposphere north of 30°N, where biomass burning signals during TRACE-P were strongest [*Carmichael et al.*, 2003a; *Liu et al.*, 2003; *Li et al.*, 2003]. Reducing Southeast Asian biomass burning emissions by 74% worsens the modeled CO_2 underestimate in the free troposphere by 0.15 ppm in comparison to the decreased biosphere/a posteriori CO simulation (model bias changes from −0.5 to −0.65 ppm). The effect on mean modeled CO_2/CO in this region is negligible (decrease of <2 mol/mol). These relatively small effects yield inconclusive results on the implied biomass burning decrease within our analysis framework. A formal coupled inversion of CO_2 and CO may better identify which scenarios are robustly constrained by the measurements. For now, our best-case scenario remains the decreased biosphere/a posteriori CO of section 6.2.

[47] The results from our best case scenario of east Asian CO_2 emissions can be compared to those of *Vay et al.* [2003], who used their TRACE-P CO_2 measurements to estimate CO_2 export fluxes from Asia for March–April, 2001. They calculated export fluxes as the product of gridded zonal wind vectors and CO_2 enhancements over a background value for the NW Pacific (20°–40°N, 120°–150°E, and 0–12 km). Two separate fluxes were calculated: (1) relative to a fixed background concentration and (2) relative to a latitudinally varying background. *Vay et al.* [2003] argue that using a fixed background yields a total CO_2 export from the Asian continent (13.93 Tg C/d), while using a latitudinally varying background yields the anthropogenic component of that export (6.37 Tg C/d). They conclude that 54% of the total east Asian CO_2 outflow is from biospheric sources. In comparison, our decreased biosphere/a posteriori CO scenario yields total CO_2 emissions for the east Asian region (as defined in Figure 3) of 13.1 Tg C/d with a biospheric contribution of 40%. The difference between the two estimates is not large, and we note that use of *Streets et al.*'s [2003] estimates of east Asian anthropogenic emissions (7.4 Tg C/d), instead of Vay et al.'s own estimate (6.4), yields a biospheric contribution of 47% in their calculation, which is closer to our estimate of 40%.

[48] The focus of this study has been to demonstrate the use of observed CO_2/CO correlations in providing top-down constraints to distinguish components of the regional CO_2 budget. We emphasize that the decrease in modeled biospheric fluxes implied by the observed CO_2/CO correlations and concentrations in this analysis is specific to the Chinese region in March 2001; it does not reflect on the accuracy of the CASA flux inventory on seasonal timescales and continental spatial scales.

7. Summary

[49] We have used observed CO_2/CO correlations in Asian outflow from the TRACE-P aircraft campaign (March–April 2001) to constrain different regional components of the east Asian CO_2 budget. The combustion sources of CO_2 and CO display characteristic emission ratios ranging from 12 mol/mol for biomass burning to over 100 for Japanese fossil fuel combustion. The biospheric source of CO_2 is almost independent of CO as the biogenic source of CO is small. These signatures yield regionally distinct emission ratios which reflect the relative proportions of the various sources within each region.

[50] Examination of boundary layer CO_2/CO correlations from individual TRACE-P flights indicates indeed distinct regional signatures. Outflow from northeast China has a low CO_2/CO slope (10–20 mol/mol), influenced by inefficient combustion sources from domestic coal and biofuel. Measurements over Japan indicate much higher slopes (60–80 mol/mol) reflecting CO emissions controls in that country.

[51] We used a global 3-D simulation of CO_2 and CO from the GEOS-CHEM model to interpret the observed CO_2/CO slopes in terms of specific sources. When driven by our best a priori estimates of sources (*Streets et al.*'s [2003] anthropogenic inventory, *Duncan et al.*'s [2003] biomass burning inventory, and the CASA biospheric model), the model overestimates both CO_2 concentrations and CO_2/CO slopes in the Chinese outflow. This implies that the regional springtime biospheric source of CO_2 from the CASA model is too high. Reconciliation of model CO_2 concentrations with the TRACE-P observations is achieved by decreasing net biospheric emissions in China by 45%

and in boreal Asia by 10%, an adjustment which is within the range of uncertainty of the CASA model fluxes. This change alone, however, is insufficient to reconcile the modeled boundary layer CO_2/CO slopes with observations. Previous analyses of the TRACE-P CO data had found that Chinese anthropogenic CO emissions must be higher than in *Streets et al.*'s [2003] inventory (by 54% according to formal inverse model analysis by *Palmer et al.* [2003a]). We find that such an adjustment improves the simulation of the CO_2/CO slopes. The analysis of *Palmer et al.* [2003a] also calls for a 74% decrease of biomass burning CO emissions from Southeast Asia relative to the a priori inventory of *Duncan et al.* [2003], but the corresponding signal in CO_2 along the TRACE-P aircraft flight tracks is too weak to provide independent information on this issue.

[52] Analysis of our CO_2 simulation indicates that a combination of factors, including underreporting of sector activity (domestic and industrial combustion) together with low bias in CO emission factors, is likely responsible for the underestimate of Chinese anthropogenic CO emissions in *Streets et al.*'s [2003] inventory. Under reporting of sector activity would imply increases in Chinese anthropogenic CO_2 emissions and would require further decrease of the Chinese biospheric CO_2 source to reconcile simulated and observed concentrations of CO_2 in the Asian outflow. Such an adjustment would still be within the uncertainty bounds on the springtime CASA fluxes. An optimal set of emissions adjustments to match the combined constraints from observed CO_2 and CO concentrations as well as CO_2:CO correlations will require a more formal inverse analysis.

[53] **Acknowledgments.** This research was funded by the NASA Carbon Cycle Program and the NASA Global Tropospheric Chemistry Program. We thank Jim Randerson, Guido van der Werff, and Seth Olsen for access to and discussions on CASA model fluxes. We thank two anonymous reviewers for helpful suggestions on improving the manuscript.

References

Anderson, B., G. Gregory, J. Collins Jr., G. Sachse, T. Conway, and G. Whiting (1996), Airborne observations of spatial and temporal variability of tropospheric carbon dioxide, *J. Geophys. Res.*, *101*, 1985–1998.

Andreae, M. O., and P. Merlet (2001), Emission of trace gases and aerosols from biomass burning, *Global Biogeochem. Cycles*, *15*, 955–966.

Bartlett, K. B., G. W. Sachse, T. Slate, C. Harward, and D. R. Blake (2003), Large-scale distribution of CH_4 in the western North Pacific: Sources and transport from the Asian continent, *J. Geophys. Res.*, *108*(D20), 8807, doi:10.1029/2002JD003076.

Bender, M., T. Ellis, P. Tans, R. Francey, and D. Lowe (1996), Variability in the O_2/N_2 ratio of Southern Hemisphere air, 1991–1994: Implications for the carbon cycle, *Global Biogeochem. Cycles*, *10*, 9–21.

Bey, I., D. J. Jacob, J. A. Logan, and R. M. Yantosca (2001), Asian chemical outflow to the Pacific: Origins, pathways and budgets, *J. Geophys. Res.*, *106*, 23,097–23,114.

Blake, N., et al. (2003), NMHCs and halocarbons in Asian continental outflow during the Transport and Chemical Evolution over the Pacific (TRACE-P) Field Campaign: Comparison With PEM-West B, *J. Geophys. Res.*, *108*(D20), 8806, doi:10.1029/2002JD003367.

Bousquet, P., P. Ciais, P. Peylin, M. Ramonet, and P. Monfray (1999), Inverse modeling of annual atmospheric CO_2 sources and sinks: 1. Method and control inversion, *J. Geophys. Res.*, *104*, 26,161–26,178.

Bousquet, P., P. Peylin, P. Ciais, C. Le Quéré, P. Friedlingstein, and P. P. Tans (2000), Regional changes of CO_2 fluxes over land and oceans since 1980, *Science*, *290*, 1342–1346.

Bradsher, K. (2003), China's boom adds to global warming problem, *New York Times*, Oct. 22 .

Carmichael, G. R., et al. (2003a), Regional-scale chemical transport modeling in support of the analysis of observations obtained during the TRACE-P experiment, *J. Geophys. Res.*, *108*(D21), 8823, doi:10.1029/2002JD003117.

Carmichael, G. R., et al. (2003b), Evaluating regional emission estimates using the TRACE-P observations, *J. Geophys. Res.*, *108*(D21), 8810, doi:10.1029/2002JD003116.

Climate Monitoring and Diagnostics Laboratory (CMDL) (2003), GLOBALVIEW-CO_2, Cooperative Atmospheric Data Integration Project–Carbon Dioxide [CD-ROM], NOAA, Boulder, Colo. (Also available at ftp.cmdl.noaa.gov, Path: Ccg/co2/GLOBALVIEW)

Cooper, O. R., J. L. Moody, D. D. Parrish, M. Trainer, T. B. Ryerson, J. S. Holloway, G. Hübler, F. C. Fehsenfeld, and M. J. Evans (2002), Trace gas composition of midlatitude cyclones over the western North Atlantic Ocean: A conceptual model, *J. Geophys. Res.*, *107*(D7), 4056, doi:10.1029/2001JD000901.

Duncan, B. N., R. V. Martin, A. C. Staudt, R. Yevich, and J. A. Logan (2003), Interannual and seasonal variability of biomass burning emissions constrained by satellite observations, *J. Geophys. Res.*, *108*(D2), 4100, doi:10.1029/2002JD002378.

Fan, S., M. Gloor, J. Mahlman, S. Pacala, J. Sarmiento, T. Takahashi, and P. Tans (1998), A large terrestrial carbon sink in North America implied by atmospheric and oceanic carbon dioxide data and models, *Science*, *282*, 442–446.

Field, C. B., J. T. Randerson, and C. M. Malmstrom (1995), Global net primary production—Combining ecology and remote-sensing, *Remote Sens. Environ.*, *51*, 74–88.

Francey, R., P. Rayner, R. Langenfelds, and C. Trudinger (1999), The inversion of atmospheric CO_2 mixing ratios and isotopic composition to constrain large-scale air-sea fluxes, paper presented at 2nd International Symposium CO_2 in the Oceans, Cent. for Global Environ. Res., Natl. Inst. for Environ. Study, Tsukuba, Japan.

Fuelberg, H. E., C. M. Kiley, J. R. Hannan, D. J. Westberg, M. A. Avery, and R. E. Newell (2003), Meteorological conditions and transport pathways during the Transport and Chemical Evolution over the Pacific (TRACE-P) experiment, *J. Geophys. Res.*, *108*(D20), 8782, doi:10.1029/2002JD003092.

Gloor, M., S.-M. Fan, S. Pacala, and J. L. Sarmiento (2000), Optimal sampling of the atmosphere for purpose of inverse modeling: A model study, *Global Biogeochem. Cycles*, *14*, 407–428.

Gurney, K. R., et al. (2002), Towards robust regional estimates of CO_2 sources and sinks using atmospheric transport models, *Nature*, *415*, 626–630.

Gurney, K. R., et al. (2004), Transcom 3 inversion intercomparison: Model mean results for the estimation of seasonal carbon sources and sinks, *Global Biogeochem. Cycles*, *18*, GB1010, doi:10.1029/2003GB002111.

Hannan, J. R., H. Fuelberg, J. Crawford, G. Sachse, and D. Blake (2003), The role of wave cyclones in transporting boundary layer air to the free troposphere during the spring 2001 NASA/TRACE-P Experiment, *J. Geophys. Res.*, *108*(D20), 8785, doi:10.1029/2002JD003105.

Heald, C. L., D. J. Jacob, P. I. Palmer, M. J. Evans, G. W. Sachse, H. B. Singh, and D. R. Blake (2003a), Biomass burning emission inventory with daily resolution: Application to aircraft observations of Asian outflow, *J. Geophys. Res.*, *108*(D21), 8811, doi:10.1029/2002JD003082.

Heald, C. L., et al. (2003b), Asian outflow and trans-Pacific transport of carbon monoxide and ozone pollution: An integrated satellite, aircraft, and model perspective, *J. Geophys. Res.*, *108*(D24), 4804, doi:10.1029/2003JD003507.

Hirsch, R. M., and E. J. Gilroy (1984), Methods of fitting a straight line to data: Examples in water resources, *Water Resour. Bull.*, *20*, 705–711.

Houghton, R. A., and J. L. Hackler (1999), Emissions of carbon from forestry and land-use change in tropical Asia, *Global Change Biol.*, *5*, 481–492.

Jacob, D. J., J. H. Crawford, M. M. Kleb, V. S. Connors, R. J. Bendura, J. L. Raper, G. W. Sachse, J. C. Gille, L. Emmons, and C. L. Heald (2003), Transport and Chemical Evolution over the Pacific (TRACE-P) aircraft mission: Design, execution, and first results, *J. Geophys. Res.*, *108*(D20), 9000, doi:10.1029/2002JD003276.

Jaeglé, L., D. A. Jaffe, H. U. Price, P. Weiss-Penzias, P. I. Palmer, M. J. Evans, D. J. Jacob, and I. Bey (2003), Sources and budgets for CO and O_3 in the northeastern Pacific during the spring of 2001: Results from the PHOBEA-II Experiment, *J. Geophys. Res.*, *108*(D20), 8802, doi:10.1029/2002JD003121.

Kasibhatla, P., A. Arellano, J. A. Logan, P. I. Palmer, and P. Novelli (2002), Top-down estimate of a large source of atmospheric carbon monoxide associated with fuel combustion in Asia, *Geophys. Res. Lett.*, *29*(19), 1900, doi:10.1029/2002GL015581.

Keeling, R. F., S. C. Piper, and M. Heimann (1996), Global and hemispheric CO_2 sinks deduced from changes in atmospheric O_2 concentration, *Nature*, *381*, 218–221.

Kiley, C. M., et al. (2003), An intercomparison and evaluation of aircraft-derived and simulated CO from seven chemical transport models during the TRACE-P experiment, *J. Geophys. Res.*, *108*(D21), 8819, doi:10.1029/2002JD003089.

Langenfelds, R. L., R. J. Francey, B. C. Pak, L. P. Steele, J. Lloyd, C. M. Trudinger, and C. E. Allison (2002), Interannual growth rate variations of atmospheric CO_2 and its $d^{13}C$, H_2, CH_4, and CO between 1992 and 1999 linked to biomass burning, *Global Biogeochem. Cycles*, *16*(3), 1048, doi:10.1029/2001GB001466.

Levine, J. (1994), Biomass burning and the production of greenhouse gases, in *Climate Biosphere Interaction: Biogenic Emissions and the Environmental Effects of Climate Change*, edited by R. G. Zepp, pp. 139–160, John Wiley, Hoboken, N. J.

Li, Q., D. J. Jacob, R. M. Yantosca, C. L. Heald, H. B. Singh, M. Koike, Y. Zhao, G. W. Sachse, and D. G. Streets (2003), A global three-dimensional model analysis of the atmospheric budgets of HCN and CH_3CN: Constraints from aircraft and ground measurements, *J. Geophys. Res.*, *108*(D21), 8827, doi:10.1029/2002JD003075.

Liu, H., D. J. Jacob, I. Bey, R. M. Yantosca, B. N. Duncan, and G. W. Sachse (2003), Transport pathways for Asian pollution outflow over the Pacific: Interannual and seasonal variations, *J. Geophys. Res.*, *108*(D20), 8786, doi:10.1029/2002JD003102.

Ma, Y., et al. (2003), Characteristics and influence of biosmoke on the fine-particle ionic composition measured in Asian outflow during the Transport and Chemical Evolution Over the Pacific (TRACE-P) experiment, *J. Geophys. Res.*, *108*(D21), 8816, doi:10.1029/2002JD003128.

Manning, A. C. (2001), Temporal variability of atmospheric oxygen from both continuous measurements and a flask sampling network: Tools for studying the global carbon cycle., Ph. D. thesis, 190 pp., Univ. of Calif., San Diego, La Jolla.

Martin, R. V., D. J. Jacob, R. M. Yantosca, M. Chin, and P. Ginoux (2003), Global and regional decreases in tropospheric oxidants from photochemical effects of aerosols, *J. Geophys. Res.*, *108*(D3), 4097, doi:10.1029/2002JD002622.

Mauzerall, D. L., J. A. Logan, D. J. Jacob, B. E. Anderson, D. R. Blake, J. D. Bradshaw, B. Heikes, G. W. Sachse, H. Singh, and B. Talbot (1998), Photocemistry in biomass burning plumes and implications for tropospheric ozone over the tropical South Atlantic, *J. Geophys. Res.*, *103*, 8401–8423.

McKeen, S. A., and S. C. Liu (1993), Hydrocarbon ratios and photochemical jistory of air masses, *Geophys. Res. Lett.*, *20*, 2362–2366.

Miyazaki, Y., et al. (2003), Synoptic scale transport of reactive nitrogen over the western Pacific in spring, *J. Geophys. Res.*, *108*(D20), 8788, doi:10.1029/2002JD003248.

Olsen, S. C., and J. T. Randerson (2004), Differences between surface and column atmospheric CO_2 and implications for carbon cycle research, *J. Geophys. Res.*, *109*, D02301, doi:10.1029/2003JD003968.

Palmer, P. I., D. J. Jacob, D. B. A. Jones, C. L. Heald, R. M. Yantosca, J. A. Logan, G. W. Sachse, and D. G. Streets (2003a), Inverting for emissions of carbon monoxide from Asia using aircraft observations over the western Pacific, *J. Geophys. Res.*, *108*(D21), 8828, doi:10.1029/2003JD003397.

Palmer, P. I., D. J. Jacob, L. J. Mickley, D. R. Blake, G. W. Sachse, H. E. Fuelberg, and C. M. Kiley (2003b), Eastern Asian emissions of anthropogenic halocarbons deduced from aircraft concentration data, *J. Geophys. Res.*, *108*(D24), 4753, doi:10.1029/2003JD003591.

Pétron, G., C. Granier, B. Khattatov, J.-F. Lamarque, V. Yudin, J.-F. Müller, and J. Gille (2002), Inverse modeling of carbon monoxide surface emissions using Climate Monitoring and Diagnostics Laboratory network observations, *J. Geophys. Res.*, *107*(D24), 4761, doi:10.1029/2001JD001305.

Peylin, P., D. Baker, J. Sarmiento, P. Ciais, and P. Bousquet (2002), Influence of transport uncertainty on annual mean and seasonal inversions of atmospheric CO_2 data, *J. Geophys. Res.*, *107*(D19), 4385, doi:10.1029/2001JD000857.

Potosnak, M. J., S. C. Wofsy, A. S. Denning, T. J. Conway, and D. H. Barnes (1999), Influence of biotic exchange and combustion sources on atmospheric CO_2 concentrations in New England from observations at a forest flux tower, *J. Geophys. Res*, *104*, 9561–9569.

Potter, C. S., J. T. Randerson, C. B. Field, P. A. Matson, P. M. Vitousek, H. A. Mooney, and S. A. Klooster (1993), Terrestrial ecosystem production: A process model based on global satellite and surface data, *Global Biogeochem. Cycles*, *7*, 811–841.

Randerson, J. T., M. V. Thompson, T. J. Conway, I. Y. Fung, and C. B. Field (1997), The contribution of terrestrial sources and sinks to trends in the seasonal cycle of atmospheric carbon dioxide, *Global Biogeochem. Cycles*, *11*, 535–560.

Rayner, P. J., I. G. Enting, R. J. Francey, and R. L. Langenfelds (1999), Reconstructing the recent carbon cycle from atmospheric CO_2, $\delta^{13}C$ and O_2/N_2 observations, *Tellus*, *Ser. B*, *51*(2), 213–232.

Russo, R., et al. (2003), Chemical composition of Asian continental outflow over the western Pacific: Results from Transport and Chemical Evolution over the Pacific (TRACE-P), *J. Geophys. Res.*, *108*(D20), 8804, doi:10.1029/2002JD003184.

Sachse, G. W., G. F. Hill, L. O. Wade, and M. G. Perry (1987), Fast-response, high-precision carbon monoxide sensor using a tunable diode laser absorption technique, *J. Geophys. Res.*, *92*, 2071–2081.

Simpson, I. J., N. J. Blake, D. R. Blake, E. Atlas, F. Flocke, J. H. Crawford, H. E. Fuelberg, C. M. Kiley, S. Meinardi, and F. S. Rowland (2003), Photochemical production and evolution of selected C_2–C_5 alkyl nitrates in tropospheric air influenced by Asian outflow, *J. Geophys. Res.*, *108*(D20), 8808, doi:10.1029/2002JD002830.

Streets, D. G., et al. (2003), An inventory of gaseous and primary aerosol emissions in Asia in the year 2000, *J. Geophys. Res.*, *108*(D21), 8809, doi:10.1029/2002JD003093.

Suntharalingam, P., C. M. Spivakovsky, J. A. Logan, and M. B. McElroy (2003), Estimating the distribution of terrestrial CO_2 sources and sinks from atmospheric measurements: Sensitivity to configuration of the observation network, *J. Geophys. Res.*, *108*(D15), 4452, doi:10.1029/2002JD002207.

Takahashi, T., et al. (1999), Net sea-air CO2 flux over the global oceans, in *Proceedings 2nd International Symposium CO_2in the Oceans: CGER-I037–'99*, pp. 9–15, Natl. Inst. for Environ. Stud., Tsukuba.

Vay, S. A., et al. (2003), Influence of regional-scale anthropogenic emissions on CO_2 distributions over the western North Pacific, *J. Geophys. Res.*, *108*(D20), 8801, doi:10.1029/2002JD003094.

Weber, R. J., et al. (2003), New particle formation in anthropogenic plumes advecting from Asia observed during TRACE-P, *J. Geophys. Res.*, *108*(D21), 8814, doi:10.1029/2002JD003112.

Yevich, R., and J. A. Logan (2003), An assessment of biofuel use and burning of agricultural waste in the developing world, *Global Biogeochem. Cycles*, *17*(4), 1095, doi:10.1029/2002GB001952.

M. J. Evans, D. J. Jacob, J. A. Logan, P. I. Palmer, P. Suntharalingam, Y. Xiao, and R. M. Yantosca, Division of Engineering and Applied Sciences, Harvard University, Pierce Hall, 29, Oxford St., Cambridge, MA 02138, USA. (mje@io.harvard.edu; djj@io.harvard.edu; jal@io.harvard.edu; pip@io.harvard.edu; pns@io.harvard.edu; xyp@io.harvard.edu; bmy@io.harvard.edu)

G. W. Sachse and S. L. Vay, NASA Langley Research Center, Mail Stop 472, VA 23681, USA. (g.w.sachse@larc.nasa.gov; s.a.vay@larc.nasa.gov)

D. G. Streets, Argonne National Laboratory, 9700 South Cass Avenue, Argonne, IL 60439, USA. (dstreets@anl.gov)